On the synergistic interaction of an ionic liquid and biopolymers in the synthesis of strontium niobate

Omar Gomez[a,b], Simon R. Hall*[a,b]

a. *Bristol Centre for Functional Nanomaterials, University of Bristol, BS8 1FD*

b. *Complex Functional Materials Group, School of Chemistry, University of Bristol, BS8 1TS.*

Abstract

The wide range of interesting properties that metal oxides exhibit has always driven creative research in this area. Here we analyse the interaction between an ionic liquid, 1-Ethyl-3-methylimidazolium acetate (emim)OAc, and biopolymers such as cellulose, chitosan, starch and dextran and demonstrate how they are intimately involved in the control of shape, size and crystallinity of strontium niobate.

Keywords: Ionic liquid; Biopolymers; Metal oxides

1. Introduction

Inorganic oxides feature prominently in biomineralization; the organic-inorganic interaction has developed over millions of years to produce optimum structures for structural support, buoyancy control and defence mechanisms in shells, corals sponges and fishes [1,2]. From those bioinorganic materials, to complex metal oxides, research has been extensive due to the wide range of possible applications that these materials possess. One reason for such diversity is due to the high tunability of the properties, which can be modified by altering factors such as the porosity, crystallinity, morphology, doping or particle size [3-6].

In nature, as in the laboratory, these physical properties can be controlled by the organic phase. Proteins and polysaccharides possess a plethora of structures and functionality, which can be used to influence the growth of the inorganic phase. An additional influence above and beyond the merely structural, is the influence of the functional side-group of the biopolymer, i.e. hydroxyls (agar, starch, cellulose), carboxyls (pectin, alginate), amide/amines (chitin/ chitosan) and sulfate (carrageenan) [7]. The interaction, both structural and chemical, with the inorganic phase invariably produces structure at the nano- and micro-scale. By judicious selection of the organic phase, laboratory-grown inorganic materials with structures such as nanocrystals, nanorods, nanoplatelets nanofibres or aerogels can be produced. [8-12]

A great deal of work has gone into understanding and establishing the optimal conditions for the synthesis of metal oxides using polysaccharides [13], however, recent works using ionic liquids to chelate metal cations with the support of these organic compounds have opened up new synthetic pathways. An Ionic liquid (IL) is a mixture of long-chain cations and coordinating anions [14]. These solvents are described as green, being environmentally friendly and able to solvate inorganic salts [15]. Some properties that make them worth of consideration are; good thermal stability, tuneable solubility, low vapour pressure [16], as well as enabling fast mass transport. ILs have been used to synthesize diverse metal oxides with a wide range of physical properties [17]. ILs can even be considered to play a role in sol-gel chemistry, as they can dissolve polymers

to form a gel structure, particularly in the case of biopolymers such as dextran, chitosan, cellulose, and starch. As both ILs and biopolymers have been used previously in the synthesis of inorganic phases, the chelating properties of both individually has been gauged, yet the interaction between the ionic liquid and those polysaccharides have not yet been studied. Here we assess the contribution of the biopolymer in an inorganic synthetic process involving an IL and how aspects of crystal structure such as size, morphology and composition differ. We have limited the use of polysaccharides to what we consider some of the most commonly used for metal oxide synthesis, namely the biopolymers dextran, chitosan, cellulose, and starch.
In this work, samples were prepared using strontium nitrate (99 %), niobium ethoxide (99.95 %), 1-Ethyl-3-methylimidazolium acetate (emim)OAc (95 %), dextran from *Leuconostoc* sp. (molecular weight 70,000 Da), chitosan (from shrimp shells, practical grade), starch (soluble, ACS reagent), and cellulose (microcrystalline, powder). All materials were purchased from Sigma-Aldrich UK. Deionized water was obtained using a MilliQ PureLab Ultra (18.2 M Ω cm-1). None of the materials required further purification and were used as received.
A typical synthetic procedure was: Strontium nitrate (99 %) (1 mL, 0.1 M) was added to 1 mL (emim)OAc under stirring and heated at 70 °C in an alumina crucible for 2 hours to ensure dehydration of the precursor. 25.1 µl of Niobium ethoxide (99.95 %) was then added and remain under stirring and heat for another 30 minutes. Finally, the organic source, 0.1 g and 1.0 g, was added to form a paste-like mixture and put in the furnace immediately to start the calcination process, which involved a heating ramp rate of 5 °C/min at 1000 °C for 2 hours dwelling time. The target stoichiometry for all syntheses was $Sr_5Nb_4O_{15}$. The characterization such as description of phase type and purity was done via X-ray diffraction (XRD), and energy dispersive X-ray analysis (EDXA) with transmission electron microscopy (SEM). TEM analysis was carried out on JEOL JEM 1400EX microscope. SEM samples analysed on JEOL JSM 5600LV with Oxford energy dispersive X-Ray (EDX). X-ray diffraction (XRD) was carried out on Bruker D8 Advance diffractometer (CuK α 1 radiation at λ = 1.54056 Å) equipped with a Lynx-eye position sensitive detector.

2. Ionic liquid

The synthesis without any complexing agent other than the ionic liquid (emim)OAc resulted in crystallites with a wide range of morphologies, both in macrostructure and at the nanoscale (Figure 1 a,b). In addition to the target phase $Sr_5Nb_4O_{15}$, we additionally observed the closely-related $Sr_2Nb_2O_7$ phase (Figure 1 c). Thus, for the ionic liquid alone, neither phase-purity nor morphological control is achieved.

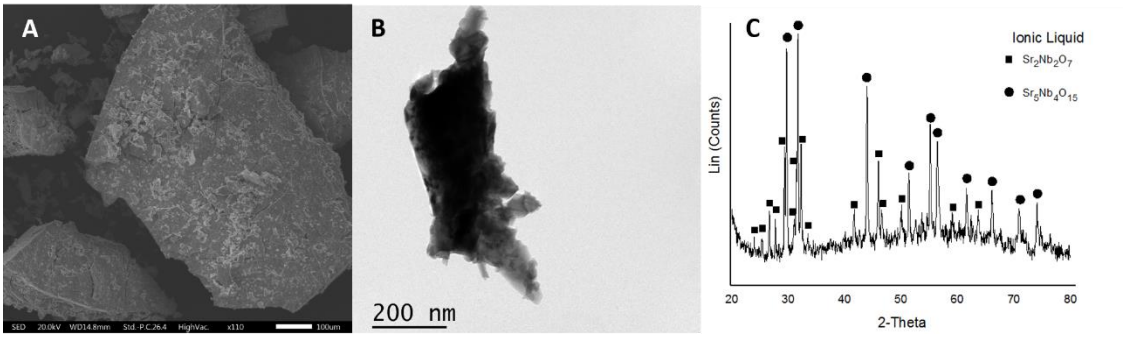

Fig. 1 (A) SEM and (B) TEM images with (C) the corresponding powder X-ray diffraction pattern from the synthesis of $Sr_5Nb_4O_{15}$ using the ionic liquid (emim)OAc as chelating agent.

3. Ionic liquid with cellulose

Cellulose is a polymeric chain composed of β(1→4) linked D-glucose units[13]. Cellulose has been used previously as a morphological agent, with fibers [18] cubic-like particles[19] or rods[20] being observed when it is incorporated into syntheses. In the case of the synthesis of $Sr_5Nb_4O_{15}$, using cellulose as an extra chelating agent provided contrasting results. When 0.1 g was used, the outcome was agglomerated crystallites that ranged in size from 100 µm to 300 µm. However, astonishing differences were seen when 1.0 g of cellulose was used. In this case, TEM images showed well-defined morphologies such as plate- and rod-like particles (Figure 2 and Supplementary information, S1). The X-ray analysis showed that with 0.1 g, a pure phase was the result, however, when 1.0 g was used, solidification of the cellulose resulted in a heterogeneous material prior to calcination. This resulted in the formation of a secondary phase, namely $Sr_2Nb_2O_7$ (Figure 2).

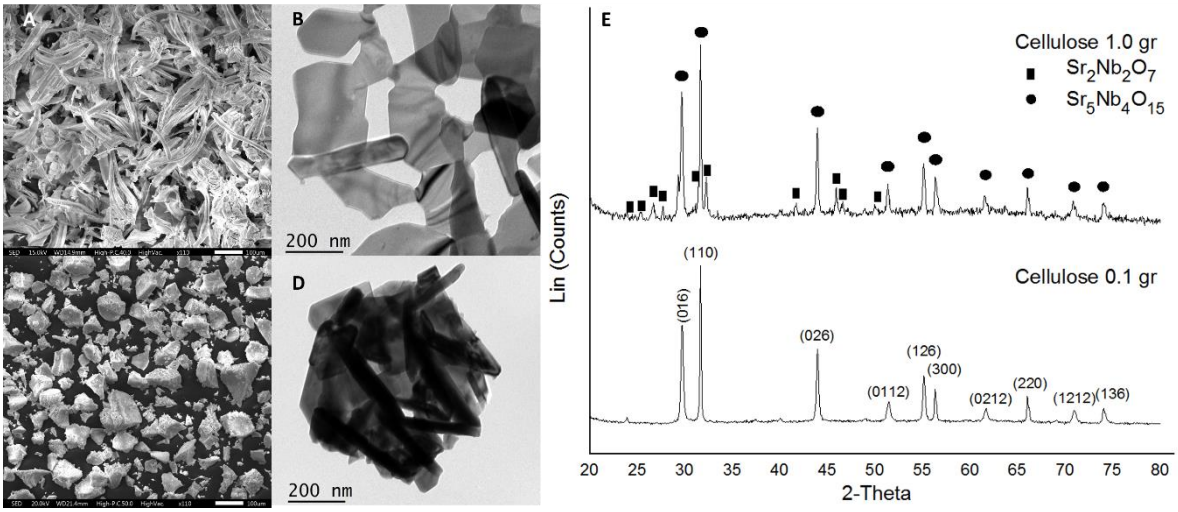

Fig. 2 (A) SEM and (B) TEM images with the corresponding powder X-ray diffraction pattern (E, top pattern) from the synthesis of $Sr_5Nb_4O_{15}$ using ionic liquid and 1 g of cellulose. (C) and (D) show SEM and TEM images respectively, with the corresponding powder X-ray diffraction pattern (E, lower pattern) from the synthesis of $Sr_5Nb_4O_{15}$ using the ionic liquid and 0.1 g of cellulose. Indexed planes correspond to the phase $Sr_5Nb_4O_{15}$.

4. Ionic liquid with chitosan

Chitosan is a high molecular weight linear polymer of 2-acetamido-2-deoxy-d-glucopyranose units linked together by 1,4-glycosidic bonds, obtained by the deacetylation of chitin. Chitin originates in fungi and exoskeletons of insects and crustaceans [13]. The most relevant feature of chitosan is the possession of NH_2 groups which might vary the reactivity and chemistry significantly when compared to other polysaccharides. In terms of micromorphology, syntheses performed with 0.1 g of chitosan as chelating agent resulted in a plate-like morphology. When 1.0 g was used however, a blocky morphology was evident. Under TEM, using 0.1 g, the sample displayed dazzling plates shadowed by spherical crystallites of smaller-scale with an average size of 20 to 30 nm (Supplementary information, S2). However, when the amount was increased to 1.0 g, the plate-like crystals commute almost exclusively to clusters of spheres. Chitosan at low doses formed plates also with small spherical crystallites, however the uniform gel structure is heavily disrupted at high concentrations and only sphere-like crystals where synthesized. This could be attributed to the fact that an excess of this organic compound physically forms crumbs (Supplementary information figure S3) instead of an evenly and uniform gel, generating multiple sites for the reaction to occur. Powder X-ray diffraction shows that at low concentrations, the addition of chitosan also provides a pure crystal phase. At high concentrations however, the pattern does change drastically. EDX analysis offers valuable information that could explain such change. Apart from the physical limitation by forming crumbs, in both cases, either low or high concentration of this compound, the elemental analysis indicated the presence of impurities (Supplementary information figure S4 and S6) such as Na, Ca and Al. The alumina crucible and the SEM holder are likely the sources of aluminium, with sodium and calcium coming from the chitosan. Interestingly, there are no nitrogen-containing impurities in the sample, as has been previously observed in other studies using chitosan in the production of metal oxides [21] (Figure 3).

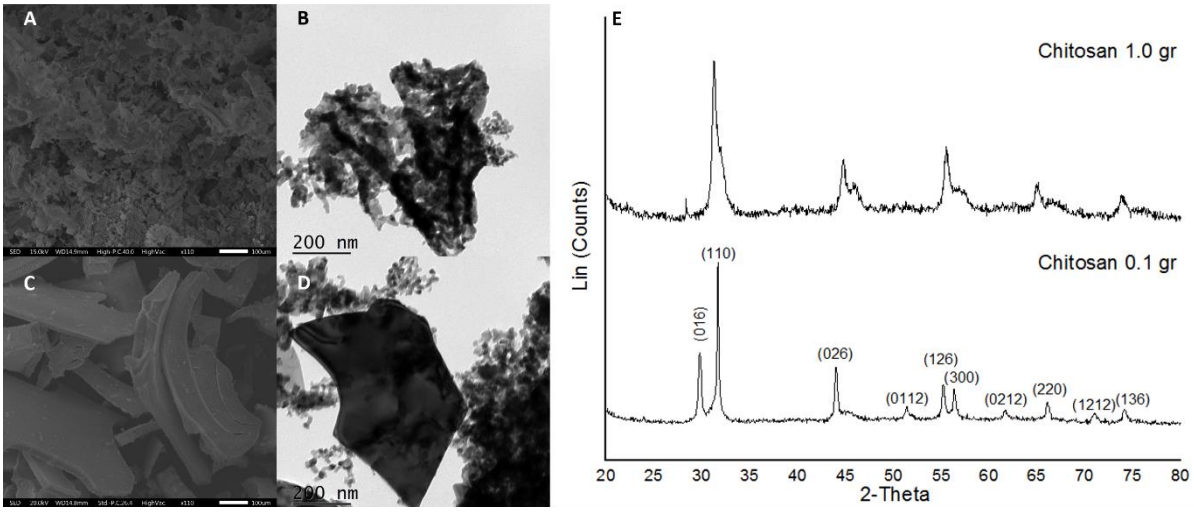

Fig. 3 (A) SEM and (B) TEM images with the corresponding powder X-ray diffraction pattern (E, top pattern) from the synthesis of $Sr_5Nb_4O_{15}$ using ionic liquid and 1 g of chitosan. (C) and (D) show SEM and TEM images respectively, with the corresponding powder X-ray diffraction pattern (E, lower pattern) from the synthesis of $Sr_5Nb_4O_{15}$ using the ionic liquid and 0.1 g of chitosan. Indexed planes correspond to the phase $Sr_5Nb_4O_{15}$.

5. Ionic liquid with starch

Starch comes from green plants and is formed by two different polymers assembled of D-glucose sequences, namely amylose and amylopectin [13]. When 0.1 g was used in the synthesis of strontium niobate, it shared a very similar crystal structure from that obtained via cellulose and the ionic liquid on its own. When the amount of the organic source is increased to 1.0 g, it showed an aggregated particle formation. In regards of the nanostructure, for both 0.1 g and 1.0 g, starch exhibited plate-like and rod-shaped crystals. In stark contrast to other biopolymers investigated here, starch seems to disrupt the chelating properties of the IL creating a mix of phases observable on the powder X-ray diffraction pattern at 1.0 g. (Figure 4) Curiously, starch has been identified as an important component in the formation of homogenous and well dispersed nanoparticles while having a relevant impact on the crystal phase [22]. Moreover, the presence of rod shape crystals has been previously reported as a main crystal structure observed when using this polysaccharide [20]. Another reason a polyphasic product is observed via X-ray diffraction is the presence of K and Ca impurities present in the starch (Supplementary information figure S5 and S6).

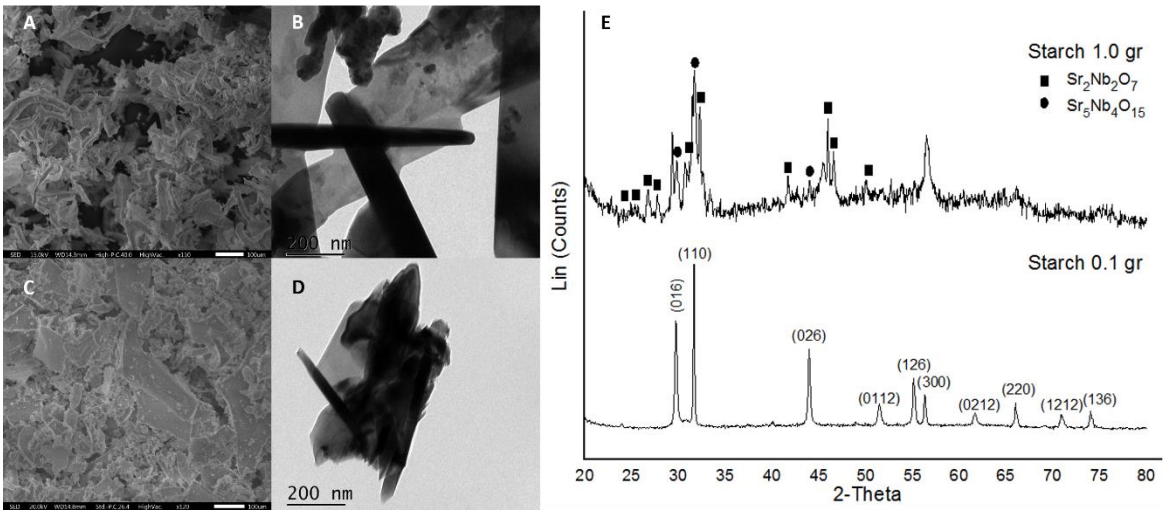

Fig. 4. (A) SEM and (B) TEM images with the corresponding powder X-ray diffraction pattern (E, top pattern) from the synthesis of $Sr_5Nb_4O_{15}$ using ionic liquid and 1 g of starch. (C) and (D) show SEM and TEM images respectively, with the corresponding powder X-ray diffraction pattern (E, lower pattern) from the synthesis of $Sr_5Nb_4O_{15}$ using the ionic liquid and 0.1 g of starch. Indexed planes correspond to the phase $Sr_5Nb_4O_{15}$.

6. Ionic liquid with dextran

Dextran is a hyper-branched polymer of dextrose of very high molecular weight obtained from the lactic-acid bacteria, with the most frequently used acquired from Leuconostoc mesenteroides and Streptococcus mutans [13]. Incorporation of dextran in the strontium niobate synthesis produced analogous morphological results to

that obtained with starch. Interestingly, dextran is the only polysaccharide that exhibited 100% pure crystalline phases at higher amounts. It has been observed previously [23] that the very high molecular weight of dextran acts as a more effective sparging agent on calcination, encouraging better mixing in the early stages of the synthesis and a totally homogeneous mixture of the precursor elements. EDX analysis also showed complete purity displaying only Sr, Nb and O in the sample (Figure 5).

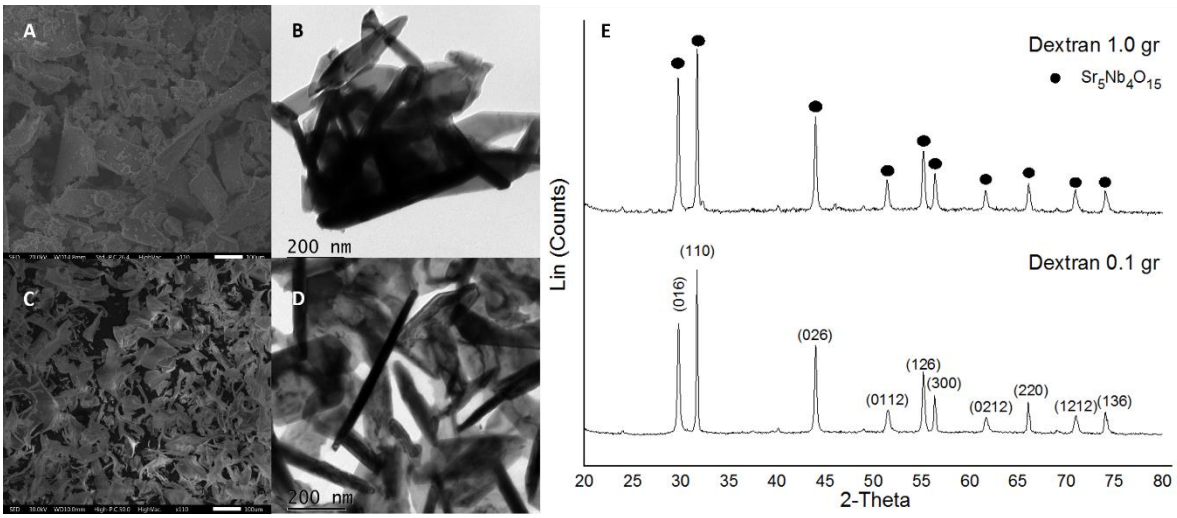

Fig. 5. (A) SEM and (B) TEM images with the corresponding powder X-ray diffraction pattern (E, top pattern) from the synthesis of $Sr_5Nb_4O_{15}$ using ionic liquid and 1 g of dextran. (C) and (D) show SEM and TEM images respectively, with the corresponding powder X-ray diffraction pattern (E, lower pattern) from the synthesis of $Sr_5Nb_4O_{15}$ using the ionic liquid and 0.1 g of dextran. Indexed planes correspond to the phase $Sr_5Nb_4O_{15}$.

7. Conclusions

The homogeneity afforded by the IL/biopolymer mixture at low concentrations clearly results in a phase-pure material through the facile mass transport of species during the synthesis. However, when the use of organic source is increased, only dextran is capable of delivering a pure phase material. This is presumably due to a disruption of mass transport through the gels. Moreover, elements presented in the organic source, such as calcium, sodium and potassium, are more evident and in enough quantities to disrupt the production of a pure phase. Furthermore, the organic source does help to lead the reaction into a specific crystal phase providing control over the stoichiometry of the reaction and the possibility to generate targeted pure phases where, on the contrary, without the organic source, a mixed phase was most commonly exhibited. Finally, the morphology of the crystals is still a task that requires further investigation, however, at low concentrations of the organic compound, in most of the cases, excepting chitosan which delivered plate-like macro and nano structures, the macromorphology and nanostructure is dictated by the ionic liquid. Interestingly morphological changes were observed when the amount of the organic source was increased, such as cellulose delivering elongated particles in both macro and nano scale, but this came at a cost to the overall phase purity of the product.

8. Conflict of interest

There are no conflicts to declare.

9. Acknowledgements

The authors would like to acknowledge the Engineering and Physical Sciences Research Council (EPSRC), UK (grant EP/G036780/1), and the Bristol Centre for Functional Nanomaterials for project funding. O.G. would like to thank Consejo Nacional de Ciencia y Tecnología (Conacyt), Mexico for the provision of a scholarship.

10. Notes and references

[1] L. Addadi, D. Joester, F. Nudelman, S. Weiner, Mollusk Shell Formation: A Source of New Concepts for Understanding Biomineralization Processes, Chem. - A Eur. J. 12 (2006) 980–987. doi:10.1002/chem.200500980.

[2] C.E. Killian, F.H. Wilt, Molecular Aspects of Biomineralization of the Echinoderm Endoskeleton, Chem. Rev. 108 (2008) 4463–4474. doi:10.1021/cr0782630.

[3] X. Chen, S.S. Mao, Titanium dioxide nanomaterials: Synthesis, properties, modifications and applications, Chem. Rev. 107 (2007) 2891–2959. doi:10.1021/cr0500535.

[4] A. Kubacka, M. Fernandez-Garcia, G. Colon, Advanced Nanoarchitectures for Solar Photocatalytic Applications, Chem. Rev. 112 (2012) 1555–1614. doi:10.1021/cr100454n.

[5] Y.-F. Sun, S.-B. Liu, F.-L. Meng, J.-Y. Liu, Z. Jin, L.-T. Kong, J.-H. Liu, Metal Oxide Nanostructures and Their Gas Sensing Properties: A Review, Sensors. 12 (2012) 2610–2631. doi:10.3390/s120302610.

[6] X. Zhao, B.M. Sanchez, P.J. Dobson, P.S. Grant, The role of nanomaterials in redox-based supercapacitors for next generation energy storage devices, Nanoscale. 3 (2011) 839. doi:10.1039/c0nr00594k.

[7] A.E. Danks, S.R. Hall, Z. Schnepp, The evolution of "sol–gel" chemistry as a technique for materials synthesis, Mater. Horiz. 3 (2016) 91–112. doi:10.1039/c5mh00260e.

[8] S. Elazzouzi-Hafraoui, Y. Nishiyama, J.-L. Putaux, L. Heux, F. Dubreuil, C. Rochas, The Shape and Size Distribution of Crystalline Nanoparticles Prepared by Acid Hydrolysis of Native Cellulose, Biomacromolecules. 9 (2008) 57–65. doi:10.1021/bm700769p.

[9] D. Klemm, F. Kramer, S. Moritz, T. Lindström, M. Ankerfors, D. Gray, A. Dorris, Nanocelluloses: A New Family of Nature-Based Materials, Angew. Chemie Int. Ed. 50 (2011) 5438–5466. doi:10.1002/anie.201001273.

[10] N. Lin, J. Huang, A. Dufresne, Preparation, properties and applications of polysaccharide nanocrystals in advanced functional nanomaterials: a review, Nanoscale. 4 (2012) 3274. doi:10.1039/c2nr30260h.

[11] S. Sarkar, E. Guibal, F. Quignard, A.K. SenGupta, Polymer-supported metals and metal oxide nanoparticles: synthesis, characterization, and applications, J. Nanoparticle Res. 14 (2012) 715. doi:10.1007/s11051-011-0715-2.

[12] P. Tingaut, T. Zimmermann, G. Sebe, Cellulose nanocrystals and microfibrillated cellulose as building blocks for the design of hierarchical functional materials, J. Mater. Chem. 22 (2012) 20105. doi:10.1039/c2jm32956e.

[13] A. Hinz, A. Schulz, A. Villinger, On the Behaviour of Biradicaloid [P(µ-NTer)]2 Towards Lewis Acids and Bases, Chem. Commun. 0 (2013) 1–3. doi:10.1039/x0xx00000x.

[14] D. Klemm, F. Kramer, S. Moritz, T. Lindstrom, M. Ankerfors, D. Gray, A. Dorris, Nanocelluloses: A New Family of Nature-Based Materials, Angew. Chemie Int. Ed. 50 (2011) 5438–5466. doi:10.1002/anie.201001273.

[15] M. Armand, F. Endres, D.R. MacFarlane, H. Ohno, B. Scrosati, Ionic-liquid materials for the electrochemical challenges of the future, Nat. Mater. 8 (2009) 621–629. doi:10.1038/nmat2448.

[16] Z. Ma, J. Yu, S. Dai, Preparation of Inorganic Materials Using Ionic Liquids, Adv. Mater. 22 (2010) 261–285. doi:10.1002/adma.200900603.

[17] D.C. Green, S. Glatzel, A.M. Collins, A.J. Patil, S.R. Hall, A New General Synthetic Strategy for Phase-Pure Complex Functional Materials, Adv. Mater. 24 (2012) 5767–5772. doi:10.1002/adma.201202683.

[18] W. Zhang, S. Chen, W. Hu, B. Zhou, Z. Yang, N. Yin, H. Wang, Facile fabrication of flexible magnetic nanohybrid membrane with amphiphobic surface based on bacterial cellulose, Carbohydr. Polym. 86 (2011) 1760–1767. doi:10.1016/j.carbpol.2011.07.015.

[19] M.A.B. Barata, M.C. Neves, C. Pascoal Neto, T. Trindade, Growth of BiVO4 particles in cellulosic fibres by in situ reaction, Dye. Pigment. 65 (2005) 125–127. doi:10.1016/j.dyepig.2004.07.005.

[20] Z. Ibupoto, K. Khun, M. Eriksson, M. AlSalhi, M. Atif, A. Ansari, M. Willander, Hydrothermal Growth of Vertically Aligned ZnO Nanorods Using a Biocomposite Seed Layer of ZnO Nanoparticles, Materials (Basel). 6 (2013) 3584–3597. doi:10.3390/ma6083584.

[21] J. Matos, P. Atienzar, H. Garcia, J.C. Hernandez-Garrido, Nanocrystalline carbon-TiO_2 hybrid hollow spheres as possible electrodes for solar cells, Carbon N. Y. 53 (2013) 169–181. doi:10.1016/j.carbon.2012.10.044.

[22] S.-J. Bao, C. Lei, M.-W. Xu, C.-J. Cai, C.-J. Cheng, C.M. Li, Environmentally-friendly biomimicking synthesis of TiO2 nanomaterials using saccharides to tailor morphology, crystal phase and photocatalytic activity, CrystEngComm. 15 (2013) 4694. doi:10.1039/c3ce40310f.

[23] D. Walsh, S.C. Wimbush, S.R. Hall, Reticulated superconducting YBCO materials of designed macromorphologies with enhanced structural stability through incorporation of lithium, Supercond. Sci. Technol. 22 (2009) 15026. doi:10.1088/0953-2048/22/1/015026.